Published in final edited form as:
Trends Neurosci. 2012 April ; 35(4): 220–229. doi:10.1016/j.tins.2011.10.007.

SENSING SOUND: MOLECULES THAT ORCHESTRATE MECHANOTRANSDUCTION BY HAIR CELLS

Piotr Kazmierczak and **Ulrich Müller**
Dorris Neuroscience Center, Department of Cell Biology, The Scripps Research Institute, La Jolla, California 92037, 858-784-7288, umueller@scripps.edu

Abstract

Animals use acoustic signals to communicate and to obtain information about their environment. The processing of acoustic signals is initiated at auditory sense organs, where mechanosensory hair cells convert sound-induced vibrations into electrical signals. Although the biophysical principles underlying the mechanotransduction process in hair cells have been characterized in much detail over the last 30 years, the molecular building blocks of the mechanotransduction machinery have proven difficult to determine. Here we review recent studies that have both identified some of these molecules and established the mechanisms by which they regulate the activity of the still-elusive mechanotransduction channel.

INTRODUCTION

Our ability to perceive sound is a demonstration of the extreme signal processing capability of the nervous system. The mammalian auditory system responds to sound-induced vibrations at atomic dimension, can amplify signals >100 fold, and has a wide dynamic range enabling us to perceive sound over a large intensity and frequency range. Changes in air pressure induce fluid motions that travel along the cochlear duct and induce mechanical vibrations at the sensory epithelium in the organ of Corti (Fig. 1A, B). As a consequence of gradual changes in the physical properties of the cochlea from the base to the apex, each segment of the sensory epithelium vibrates in response to a specific frequency. Three rows of outer hair cells (OHCs) (Fig. 1B) amplify the vibrations. The mechanical signals are then transferred onto inner hair cells (IHCs) (Fig. 1B), which transmit the information to afferent neurons. Hair cells at the base of the cochlea respond to the highest and those at the apex to the lowest frequencies. Sound frequencies are therefore relayed to the nervous system as a tonotopic map (for recent reviews, see [1-4]).

At the heart of hearing is the mechanotransduction process, the conversion of mechanical force into electrical signals. This process is carried out by the mechanosensory hair cells of the cochlea. The molecular components of the mechanotransduction machinery of hair cells have for decades escaped detection, largely because hair cells are few in numbers and hard to manipulate experimentally. As in other experimental systems, genetic studies have recently overcome these problems. The study of genes that are linked to deafness, the most common form of sensory impairment in humans, has finally led to the identification of some of the components of the mechanotransduction machinery. Here we summarize these

findings as well as several studies that have provided insights into the properties of the molecules of mechanotransduction.

AUDITORY MECHANOSENSATION: CONVERTING SOUND INTO ELECTRICAL SIGNALS

Hair bundles and tip links

The mechanically sensitive organelle of a hair cell is the hair bundle, which consists of actin-rich stereocilia that contain mechanotransduction channels close to their tips (Fig. 1C, Fig. 2A,B). Stereocilia are organized in rows of decreasing heights and are connected by extracellular filaments, including the tip and ankle links, as well as the top and shaft connectors (Fig. 2A). These linkages are remodeled during development; mature murine cochlear hair cells retain only tip links and top connectors (for recent reviews, see [3, 4]). The stereociliary bundle is polarized in the apical hair cell surface, which provides directional sensitivity to stimulation. Sound-induced deflection of the hair bundle in the direction of the longest stereocilia increases channel open probability; deflections in the opposite direction decreases channel open probability (for a recent review, see [1]).

Since their original discovery [5], tip links have been proposed to transmit tension force onto the transduction channel. In support of this model, tip links are oriented along the mechanical sensitivity axis of hair cells [5]. Furthermore, Ca^{2+} flows into sterocilia close to their tips [6, 7]. Finally, disrupting tip links by removal of Ca^{2+} or treatment with the protease elastase leads to loss of mechanosensitivity of the hair bundle [8, 9].

Coherence in motion

The hair bundle of a hair cell is exquisitely sensitive to mechanical stimulation. At the threshold of hearing, bundles are deflected by <1 nm [10, 11]; maximal response to mechanical stimulation is evoked by ~1^0 angular deflection [12]. The analysis of hair bundle motion in response to low-frequency stimulation has shown that stereocilia tilt around the pivots at their base [13-15]. Recent optical measurements with frog saccular hair cells demonstrate that the stereocilia within a bundle show a high degree of coherence in motion with little splay [16, 17]. Pretreatment of hair bundles with the Ca^{2+} chelator, BAPTA, to break tip links [16, 17], or with proteinase XXIV to remove ankle links and shaft connectors [16], does not affect coherence in motion. These treatments leave top connectors intact, suggesting that they might mediate sliding adhesion between stereocilia [16]. At small deflections, the close apposition of stereocilia immobilizes the liquid between them, which reduces drag in the bundle and suppresses the squeezing but not the sliding mode of stereociliary motion. Therefore, most stereocilia inside the bundle experience little viscous drag; their tips experience maximal force [18]. Coherence in stereociliary motion ensures excellent sensitivity to mechanical stimulation by allowing for synchronous gating of transduction channels across the bundle.

Transducer channel activation

Transduction channels open in response to mechanical stimulation within microseconds, indicating that mechanical force directly gates the channel [12, 19]. In the turtle, activation kinetics varies tonotopically [20]; it is reasonable to assume, although not experimentally verified, that tonotopic variation is a universal feature of the vertebrate cochlea, thereby matching the properties of the transduction channel to the sound frequency they process. The properties of the transducer current fit well with a model where mechanical force is transmitted to the molecular gate of the transduction channel by an elastic gating spring with a stiffness of ~ 1mN/m [12]. Deflection of the hair bundle towards the longest stereocilia increases tension in the gating spring, which promotes transition from the channel's closed

to open state (Fig. 2C) [21]. Based on the mechanical behavior of hair bundles, the length of the swing by the gate of the transduction channel is estimated to be ~4-11 nm [22, 23]. This is a relatively large displacement and might reflect conformational changes in more than one molecule.

Transducer channel adaptation

Following activation, hair cells adapt to constant mechanical stimulation. Adaptation is thought to extend the dynamic range of hair cells, contribute to their frequency selectivity, and assist in signal amplification. In the absence of mechanical stimulation, adaptation also establishes a resting current in hair cells (for recent reviews see [1, 24-26]). Adaptation progresses on a fast and slow time scale and is regulated by influx of Ca^{2+} through the transduction channel [27, 28] (Fig. 2C). Adaptation in the cochlea is faster than in the vestibule, and fast adaptation rates vary tonotopically where cells responding to higher frequencies show higher adaptation rates [20, 27, 29-35]. These features of adaptation are likely important for tuning hair cells to their specific frequencies.

Fast and slow adaptation are thought to occur by different mechanisms (Fig. 2C). Two prominent models have been proposed for fast adaptation. In one model, Ca^{2+} binds to the channel and stabilizes it in the closed state [22, 36]. Alternatively, Ca^{2+} might bind to a site near the channel, causing release of a mechanical element in series with the transduction machinery leading to decrease in tension and channel closure [37, 38]. Slow adaptation is thought to involve an adaptation motor linked to the upper insertion point of tip links. According to the model, the motor protein climbs up along F-actin, establishing tension in the transduction machinery. During mechanical stimulation, Ca^{2+} that flows into stereocilia releases the motor from F-actin, reducing tension and leading to channel closure. Subsequently, the Ca^{2+} concentration in stereocilia declines and the motor reestablishes tension (Fig. 2C) [39, 40]. As outlined below, recent studies suggest that models of slow adaptation might need revision.

THE ELUSIVE TRANSDUCTION CHANNEL

Channel numbers and properties

Despite decades of study, the hair cell's transduction channel has not been identified. The challenges to identify the channel are tremendous. Most importantly, there are few hair cells and transduction channels per animal. Hair cells also resist experimental manipulations typically used in other experimental systems. For example, hair cells are difficult to transfect, necessitating time-consuming genetic studies to verify channel candidates. However, electrophysiological recordings have shown that the transduction channel is a non-selective cation channel with a preference for Ca^{2+} [41, 42]. Best estimates suggest that there are two active channels per tip link [7, 22, 43, 44]. Studies in the turtle indicate that the channel pore is considerably larger than in other cation channels with a minimal pore diameter of ~12.5 Å [45]. In the rat, channel conductance in IHC is in the order of 260 pS; it varies tonotopically in OHCs from 145 pS at the apex and 210 pS in the mid frequency range and was estimated to be 320 pS in the high frequency range [43]. Similar tonotopic conductance changes are observed in the turtle [44], indicating that this is a conserved property of the auditory system. The conductance changes indicate that the channel might consist of several subunits with variations in subunit composition along the length of the sensory epithelium.

Channel localization and slow adaptation

Ca^{2+} imaging studies initially supported the location of the transduction channel on both tip-link ends [7], but a recent study using high-resolution imaging provided convincing

evidence that the channel is localized to the lower tip-link end [6]. The localization of the transduction channel suggests a physical connection to the tip link, but it does not necessarily have to be direct. The channels could be opened by the change in tension of the lipid bilayer, as has been suggested in other systems [46, 47]. In this model, the number of open channels depends on the distance of force propagation within the membrane; a large number of channels could be present in stereocilia as long as on average only two channels are opened simultaneously by membrane stretch.

The localization of the transduction channel raises questions regarding models of slow adaptation because it places the site of Ca^{2+} entry into stereocilia at the lower tip-link end, far away from the proposed localization of the adaptation motor at the upper tip-link end (Fig. 2C). To reconcile these differences, it has been proposed that Ca^{2+} entering through the transduction channel might affect the adaptation motor hooked up to the next tip link lower down in the same stereocilium [1]. In this scenario, adaptation motors in the longest stereocilia would experience minimal changes in Ca^{2+} and likely not show Ca^{2+}-dependent adaptation. In addition, slow adaptation rates in mammalian auditory hair cells are much faster than in vestibular hair cells and hair cells in other species [27, 32, 33, 35, 36] raising the question whether the same mechanism controls slow adaptation in all hair-cell types.

THE TIP LINK: AN UNUSAL CADHERIN ADHESION COMPLEX

Molecular constituents of tip links

The hunt for the molecular components of the tip link has been active for over 20 years. Recent studies finally have demonstrated that tip links are formed by cadherin 23 (CDH23) and protocadherin 15 (PCDH15), two cadherin superfamily members (Fig. 2B). Hints that these proteins are important in hair cells came from the observation that mutations in their genes lead to deafness [48-55]. In mice, mutations in *Cdh23* and *Pcdh15* also lead to morphological hair bundle defects [49, 53, 55], and zebrafish with mutations in *Cdh23* lack tip links [56]. Immunolocalization studies with an antibody to CDH23 demonstrated its presence at tip links [57]. Subsequently, PCDH15 was localized to tip links [58]. Using a combination of immunolocalization, biochemical and structural studies, it was finally shown that tip links are heterophilic adhesion complexes consisting of parallel CDH23 cis-homodimers interacting in trans with parallel PCDH15 cis-homodimers to form the upper and lower parts of tip links, respectively (Fig. 2B) [59]. Subsequent studies have confirmed the localization of CDH23 and PCDH15 at tip links [60].

A new adhesion mode

Like classical cadherins, tip-link cadherins each contain an ectodomain largely composed of extracellular cadherin (EC) repeats that fold into immunoglobulin-like globular domains featuring two opposed β-sheets formed by seven β-strands. Three Ca^{2+} ions bind between EC domains and stabilize cadherin structure. Classical cadherins have 5 EC repeats while the longest isoforms of CDH23 and PCDH15 have 27 and 11 EC repeats, respectively (Fig. 3A) (for recent reviews see [61-64]). Classical cadherins are Ca^{2+}-dependent homophilic receptors, albeit with some affinity for closely related family members [63, 65, 66]. They form large adhesion complexes at adherens junctions [62]. The basic adhesive unit is a trans dimer comprised of opposing monomers [67-69]. Binding is achieved through EC1, where N-terminal β-strands are swapped between binding partners (Fig. 4A,B) [67, 68]. Classical type I cadherins have one Trp residue at amino acid position 2 (W2) that fits into a hydrophobic pocket on the opposing EC1 domain, while classical type II cadherins contain two Trps (W2 and W4) that fit into two binding pockets enhancing binding affinity (Fig. 4C) [70].

The tip-link complex differs significantly from the classical cadherin complex. A tetramer consisting of two cis-homodimers interacting in trans is the functional unit [59]. Trp2/4 are not conserved in EC1. Two laboratories have solved the structure of the first 2 EC domains of CDH23 [71, 72]. The typical EC fold is maintained but a classic trans-binding interface is not (Fig. 4D,E). Instead, polar residues at the N-terminus of CDH23 form a novel Ca^{2+}-binding motif (Fig. 4E,F). The PCDH15 N-terminus also harbors polar amino acids; biochemical studies show that polar amino acids in both cadherins are required for trans binding [71]. These amino acids might be necessary for correct protein folding or could serve to integrate Ca^{2+} into the trans-binding surface, perhaps to increase adhesive strength. In classical cadherins, the trans-binding affinity is surprisingly low (e.g., mouse E-cadherin; Kd = 97 μM [73]), and adhesive strength is achieved through lateral cadherin clustering. Lateral clustering does not occur at tip links, necessitating a different mechanism for high-affinity binding that can sustain substantial mechanical force. Measurements of the affinity for interactions between CDH23 and PCDH15 are eagerly awaited.

In classical cadherins, competition between trans- and cis-binding modes mediated by EC1 is thought to reduce affinity for trans binding [63, 74]. During adherens junction formation, such competition is mitigated by a steric mechanism resulting from ectodomain curvature [63, 75]. Tip-link cadherins lack this curvature and bind heterophilically (Fig. 4D), which can be viewed as yet another mechanism to increase binding affinity.

Cis interactions by classical cadherins and tip-link cadherins

Unlike classical cadherins, which engage in cis interactions by a binding surface on EC1 that interacts with EC2 [76], the CDH23 and PCDH15 extracellular domains form parallel homodimers with extensive lateral contacts [59]. Theoretical studies have tested the hypothesis that a classical cadherin junction is an ordered, thermodynamically condensed 2D lattice of trans dimers held together by cis interactions [77, 78]. A model built on experimentally supported assumptions predicts that junction formation is a cooperative process in which initial contact between cells is mediated by trans dimers, creating a thermodynamic diffusion trap, which promotes recruitment of monomers and formation of additional trans dimers. In this model, an ordered junction can form only in the presence of cis interactions. The extensive lateral alignment between the extracellular domains of CDH23 (and PCDH15) molecules might prevent additional lateral interactions that would lead to cadherin clusters, clearly an adhesion mode not desirable for tip-link formation.

Tip links as gating springs?

Since its discovery, the tip link has been an attractive candidate for the gating spring. However, high-resolution electron microscopic (EM) images suggest that tip links are stiff and buckle under strain [79]. Modeling of the classical C-cadherin extracellular domain suggests high stiffness in the presence of Ca^{2+} and limited elasticity without Ca^{2+} [80, 81]. Modeling studies based on the structure of the CDH23 EC1-EC2 fragment attempted to provide estimates of the tip-link stiffness [72]. EC1 alone displayed stiffness of 710 mN/m; simulations with the first two EC domains produced the value of 570 mN/m Assuming similar properties for the remaining EC domains, tip-link stiffness was predicted at ~40-60 mN/m. Even when Ca^{2+} was omitted in the simulations tip-link stiffness was considerable at 16 mN/m [72], far greater than the 1 mN/m measured for the gating spring.

The values obtained by modeling are burdened with several approximations. First, calculations were based on the model derived from a monomeric EC1-EC2 fragment of CDH23. Nothing is known about the structure of the remaining 25 EC domains of CDH23 and the 11 EC domains of PCDH15. Second, the membrane proximal regions of CDH23 and PCDH15 (~100 amino acids) fold into an unknown structure. Finally, EM studies suggest

that the two strands of the tip link filament separate close to the upper membrane insertion point [79]. Such separation could lead to substantial structural flexibility.

Mechanical properties of tip-link cadherins have not been studied, but the nanomechanics of C-cadherin has been experimentally analyzed [81]. Single molecule force spectroscopy confirms Ca^{2+} induces ectodomain rigidification. When force is applied in the presence of 1 mM Ca^{2+}, EC domain unfolding requires ~186 pN and stretches the molecule by ~34.2 nm. This force peak is preceded by a smaller one. At ~143 pN C-cadherin stretches by ~2.7 nm as a single Ca^{2+} binding site unfolds. Without Ca^{2+}, the EC domains are less stable and unfold at ~83 pN [81]. At 0.1 mM Ca^{2+}, the unfolding force is ~90 pN, significantly lower than in 1 mM Ca^{2+}.[81]. Notably, the Ca^{2+} concentration of the endolymph varies tonotopically and reaches low levels (~20 micromolar) [82, 83]. Trans interactions between CDH23 and PCDH15 are not disrupted even at 100 micromolar Ca^{2+} [59], but low local Ca^{2+} concentration might affect the mechanical properties of tip-links.

Based on the above studies, it seems plausible that the gating spring is formed by a molecule distinct from tip-link cadherins, although it does not necessarily have to be a protein. The plasma membrane near the lower tip-link insertion points appears to be under tension and pulls away from the cytoskeleton; this morphological feature is lost when tip links are broken [8, 79, 84]. Perhaps, forces that are too small to rupture or stretch tip links can deform the lipid bilayer. Interestingly, the stiffness module of the plasma membrane of the cell body in OHCs is ~1 mN/m [85], a value strikingly similar to the gating-spring stiffness. We do not know the mechanical properties of the stereociliary membrane, but one possibility is that force-induced membrane deformation could account for the gating spring.

CYTOPLASMIC COMPONENTS OF THE TIP-LINK COMPLEX

Cytoplasmic domains of tip-link cadherins

The cytoplasmic domains of classical cadherins harbor binding sites for many proteins, including β-catenin and p120 catenin [69]. The cytoplasmic domains of tip-link cadherins show no sequence homology to classical cadherins, suggesting that they recruit different proteins. Both the CDH23 and PCDH15 cytoplasmic domains are also alternatively spliced, providing additional diversity. Two cytoplasmic splice variants have been described for CDH23. The longer isoform contains an insert of 35 amino acids and is specifically expressed in hair cells [57, 86]. For PCDH15, three prominent isoforms named CD1, CD2, and CD3, which differ in their cytoplasmic domains, have been described; all three are expressed in hair cells [58, 87]. However, which isoforms of CDH23 and PCDH15 contribute to the tip link is unclear (see below).

Binding partners for CDH23 and PCDH15 and hair bundle development

The identification of binding partners for the cytoplasmic domains of CDH23 and PCDH15 has been facilitated by the study of genes linked to deafness. Mutations in *CDH23* and *PCDH15* lead to Usher syndrome Type I (USH1) [48, 50-52], a severe form of deaf-blindness. The disease is also caused by mutations in the genes encoding the molecular motor myosin 7a (Myo7a), and the adaptor proteins harmonin and sans (scaffold protein containing ankyrin repeats and SAM domain) [48, 50-52, 88-90]. Mutations in murine orthologs of the human genes lead to defects in hair bundle morphology, suggesting that USH1 proteins act in a common pathway [49, 53, 55, 91-95]. This notion is supported by *in vitro* studies, which show that USH1 proteins bind to each other. Harmonin, sans and Myo7a bind *in vitro* to all USH1 proteins; harmonin and sans also interact homophilically; finally, harmonin and Myo7a bind to F-actin (for protein domain structures, see Fig. 3) [86, 95-102].

USH1 proteins are broadly distributed in developing hair bundles, where they form the linkages that connect the stereocilia to each other and to the single kinocilium (which is present in developing cochlear hair cells but degenerates as the cells mature) (for recent reviews see [3, 4]). Intriguingly, alternative splicing regulates the function of PCDH15 in hair cells. PCDH15-CD2-deficient mice, but not mice lacking PCDH15-CD1 or –CD3 lack kinociliary links and develop hair bundles with abnormal polarity [87]. PCDH15-CD2 is abundantly expressed in the kinocilium, while CDH23 is expressed in the adjacent stereocilia, suggesting that kinociliary links are heteromeric complexes consisting of CDH23 and PCDH15 [60, 87]. Therefore, kinociliary links resemble tip links in composition, except with reversed polarity in CDH23 and PCDH15 localization relative to the hair bundle polarity axis [59, 60]. PCDH15-CD2 in kinocilia might recruit CDH23, which does not traffic into kinocilia, to the longest stereocilia next to the kinocilium. This would lead to the formation of kinociliary links. Some CDH23 in the longest stereocilia might then bind to PCDH15 in the next shorter row of stereocilia, establishing opposite polarity in tip links.

Binding partners for CDH23 at tip links

The tip-link localization of CDH23 and PCDH15 suggested that their bindings partners also function in mechanotransduction. This was initially demonstrated for harmonin-b, a harmonin isoform that binds to CDH23, Myo7a, sans and F-actin [86, 96-99, 101, 102] (Fig. 5). In adult hair cells, harmonin-b is localized to the upper tip-link density (UTLD) [29], which can be visualized by transmission EM as a density below the membrane at the upper tip-link insertion-point [103]. *Deaf circler* (*dfcr*) mice, which carry a harmonin-b mutation that prevents interaction with F-actin [92], preserve their tip links but lack UTLDs [29]. Gating of transduction channels throughout the hair bundle is less well coordinated in the mutants, and transducer current activation and adaptation are slowed [29]. Harmonin-b might connect the tip link to the cytoskeleton and regulates the activity of the slow adaptation motor thereby establishing tension in the transduction machinery. Analyses of transducer currents in *dfcr2J* mice, which entirely lack harmonin-b, have similarly implicated harmonin in regulating the slow adaptation motor [104].

The most prominent current model proposes that the slow adaptation motor is formed by a cluster of myosin-1c (Myo1c) motor proteins at the UTLD (for a recent review, see [25]). In support of this model, Myo1c in frogs is concentrated close to the UTLD [105, 106]; its inactivation dramatically affects channel open probability at rest and adaptation [33, 107]. The close proximity of Myo1c and harmonin-b at UTLDs and the demonstration that Myo1c forms a protein complex with CDH23 [57], suggest that harmonin-b might affect Myo1c function. However, as outlined above (see also Fig. 2C), Ca^{2+} enters stereocilia close to the lower end of tip links [6], raising questions as to the mechanism by which Ca^{2+}regulates the slow adaptation motor at the upper tip-link end. Furthermore, a recent study shows that in IHC of mammals, Myo1c is distributed along the length of stereocilia [108]. Therefore, the function of Myo1c in adaptation needs further study.

Myo7a has emerged as a second candidate for the slow adaptation motor. Accordingly, mice with a mutation in Myo7a show defects in transduction and altered adaptation [109]. Immunolocalization studies suggested that Myo7a in frog hair cells is concentrated in the cell body and at the base of the hair bundle [110], but a study in mice has revealed additional expression at the UTLD [111]. The same study also localized sans to the UTLD [111]. Biochemical and crystallographic data show that CDH23, harmonin, Myo7a, and sans form a multimeric protein complex (Fig. 5) [86, 96-99, 101, 102, 111]. Notably, harmonin binds through multiple surfaces to CDH23 [86, 96-99, 101, 102, 111] leading to a binding affinity that is far greater than measured for interactions between other PDZ domain proteins and their interaction partners [97]. Inactivation of sans in mice leads to a reduction in transducer

current and loss of tip links [91]. Perhaps the protein complex at UTLDs is unstable without sans.

Binding partners for PCDH15 at tip links

Little is known about the putative protein complex at the lower tip-link end that includes PCDH15 and the elusive transduction channel. Immunolocalization studies initially suggested that the PCDH15-CD3 isoform is present at the lower tip-link end [58]. However, tip links form in mice individually lacking PCDH15-CD1, -CD2, and –CD3, indicating that several of these isoforms function redundantly at tip links [87]. Notably, all PCDH15 isoforms share a proline-rich membrane proximal region and contain a C-terminal binding site for PDZ domain proteins (Fig. 3) [58]. They might therefore recruit similar proteins through these shared domains. Several proteins such as whirlin, Myo3a, Myo15, and espin1 have been localized to the tips of stereocilia; functional studies implicate them in regulating stereociliary elongation (for a recent review see [4]). The extent to which these proteins participate in regulating transduction channels is unclear. Mice with mutation in Myo15 show altered transduction [112, 113], but morphological hair bundle defects make it difficult to ascertain direct effects of Myo15 on transduction. As pointed out above, structural studies and immunolocalization studies have placed sans at the UTLD, but a recent study has concluded that sans is located close to the LTLD [91]. Sans might therefore also play a role in regulating transduction at the lower tip-link region.

CONCLUDING REMARKS

Building on a solid biophysical foundation, researchers have started to identify the molecules required for mechanotransduction by hair cells. Two themes emerge: asymmetry and evolution of special features required for force transmission. Asymmetry is evident in the composition of the tip-link, in the proteins recruited by the cytoplasmic domains of tip-link cadherins, and in the localization of the transduction channel (Fig. 2). Specialized features for force transmission are likely the new binding surface between CDH23 and PCDH15, and the high-affinity binding mode between CDH23 and harmonin. However, there are a number of important outstanding questions (Box 1). The most intriguing issue, of course, is the identity of the transduction channel.

Acknowledgments

We thank members of the laboratory and Dr. Peter Gillespie (Oregon Hearing Research Center & Vollum Institute) for comments. This work was supported by funding from the National Institutes of Health (DC005965, DC007704), the California Institute of Regenerative Medicine, the Skaggs Institute for Chemical Biology, the Bundy Foundation, and the Dorris Neuroscience Center.

REFERENCES

1. Gillespie PG, Muller U. Mechanotransduction by hair cells: models, molecules, and mechanisms. Cell. 2009; 139:33–44. [PubMed: 19804752]
2. Meyer AC, Moser T. Structure and function of cochlear afferent innervation. Curr Opin Otolaryngol Head Neck Surg. 2010; 18:441–446. [PubMed: 20802334]
3. Richardson GP, et al. How the genetics of deafness illuminates auditory physiology. Annual review of physiology. 2011; 73:311–334.
4. Schwander M, et al. Review series: The cell biology of hearing. J Cell Biol. 2010; 190:9–20. [PubMed: 20624897]
5. Pickles JO, et al. Cross-links between stereocilia in the guinea pig organ of Corti, and their possible relation to sensory transduction. Hear Res. 1984; 15:103–112. [PubMed: 6436216]
6. Beurg M, et al. Localization of inner hair cell mechanotransducer channels using high-speed calcium imaging. Nat Neurosci. 2009; 12:553–558. [PubMed: 19330002]

7. Denk W, et al. Calcium imaging of single stereocilia in hair cells: localization of transduction channels at both ends of tip links. Neuron. 1995; 15:1311–1321. [PubMed: 8845155]
8. Assad JA, et al. Tip-link integrity and mechanical transduction in vertebrate hair cells. Neuron. 1991; 7:985–994. [PubMed: 1764247]
9. Zhao Y, et al. Regeneration of broken tip links and restoration of mechanical transduction in hair cells. Proc Natl Acad Sci U S A. 1996; 93:15469–15474. [PubMed: 8986835]
10. Markin VS, Hudspeth AJ. Gating-spring models of mechanoelectrical transduction by hair cells of the internal ear. Annu Rev Biophys Biomol Struct. 1995; 24:59–83. [PubMed: 7663129]
11. Rhode WS, Geisler CD. Model of the displacement between opposing points on the tectorial membrane and reticular lamina. J Acoust Soc Am. 1967; 42:185–190. [PubMed: 6052076]
12. Corey DP, Hudspeth AJ. Kinetics of the receptor current in bullfrog saccular hair cells. J Neurosci. 1983; 3:962–976. [PubMed: 6601694]
13. Crawford AC, et al. Activation and adaptation of transducer currents in turtle hair cells. J Physiol. 1989; 419:405–434. [PubMed: 2621635]
14. Flock A, et al. Studies on the sensory hairs of receptor cells in the inner ear. Acta Otolaryngol. 1977; 83:85–91. [PubMed: 842331]
15. Hudspeth AJ, Corey DP. Sensitivity, polarity, and conductance change in the response of vertebrate hair cells to controlled mechanical stimuli. Proc Natl Acad Sci U S A. 1977; 74:2407–2411. [PubMed: 329282]
16. Karavitaki KD, Corey DP. Sliding adhesion confers coherent motion to hair cell stereocilia and parallel gating to transduction channels. J Neurosci. 2010; 30:9051–9063. [PubMed: 20610739]
17. Kozlov AS, et al. Coherent motion of stereocilia assures the concerted gating of hair-cell transduction channels. Nat Neurosci. 2007; 10:87–92. [PubMed: 17173047]
18. Kozlov AS, et al. Forces between clustered stereocilia minimize friction in the ear on a subnanometre scale. Nature. 2011; 474:376–379. [PubMed: 21602823]
19. Crawford AC, et al. Activation and adaptation of transducer currents in turtle hair cells. J Physiol. 1989; 419:405–434. [PubMed: 2621635]
20. Ricci AJ, et al. The transduction channel filter in auditory hair cells. J Neurosci. 2005; 25:7831–7839. [PubMed: 16120785]
21. Shotwell SL, et al. Directional sensitivity of individual vertebrate hair cells to controlled deflection of their hair bundles. Ann N Y Acad Sci. 1981; 374:1–10. [PubMed: 6978627]
22. Howard J, Hudspeth AJ. Compliance of the hair bundle associated with gating of mechanoelectrical transduction channels in the bullfrog's saccular hair cell. Neuron. 1988; 1:189–199. [PubMed: 2483095]
23. Ricci AJ, et al. Mechanisms of active hair bundle motion in auditory hair cells. J Neurosci. 2002; 22:44–52. [PubMed: 11756487]
24. Fettiplace R, Ricci AJ. Adaptation in auditory hair cells. Curr Opin Neurobiol. 2003; 13:446–451. [PubMed: 12965292]
25. Gillespie PG, Cyr JL. Myosin-1c, the hair cell's adaptation motor. Annual review of physiology. 2004; 66:521–545.
26. Hudspeth AJ. Making an effort to listen: mechanical amplification in the ear. Neuron. 2008; 59:530–545. [PubMed: 18760690]
27. Eatock RA, et al. Adaptation of mechanoelectrical transduction in hair cells of the bullfrog's sacculus. J Neurosci. 1987; 7:2821–2836. [PubMed: 3498016]
28. Crawford AC, et al. The actions of calcium on the mechano-electrical transducer current of turtle hair cells. J Physiol. 1991; 434:369–398. [PubMed: 1708822]
29. Grillet N, et al. Harmonin mutations cause mechanotransduction defects in cochlear hair cells. Neuron. 2009; 62:375–387. [PubMed: 19447093]
30. Kennedy HJ, et al. Fast adaptation of mechanoelectrical transducer channels in mammalian cochlear hair cells. Nat Neurosci. 2003; 6:832–836. [PubMed: 12872124]
31. Ricci AJ, Fettiplace R. The effects of calcium buffering and cyclic AMP on mechano-electrical transduction in turtle auditory hair cells. J Physiol. 1997; 501(Pt 1):111–124. [PubMed: 9174998]

32. Stauffer EA, Holt JR. Sensory transduction and adaptation in inner and outer hair cells of the mouse auditory system. J Neurophysiol. 2007; 98:3360–3369. [PubMed: 17942617]
33. Stauffer EA, et al. Fast adaptation in vestibular hair cells requires Myosin-1c activity. Neuron. 2005; 47:541–553. [PubMed: 16102537]
34. Vollrath MA, Eatock RA. Time course and extent of mechanotransducer adaptation in mouse utricular hair cells: comparison with frog saccular hair cells. J Neurophysiol. 2003; 90:2676–2689. [PubMed: 12826658]
35. Waguespack J, et al. Stepwise morphological and functional maturation of mechanotransduction in rat outer hair cells. J Neurosci. 2007; 27:13890–13902. [PubMed: 18077701]
36. Wu YC, et al. Two components of transducer adaptation in auditory hair cells. J Neurophysiol. 1999; 82:2171–2181. [PubMed: 10561397]
37. Bozovic D, Hudspeth AJ. Hair-bundle movements elicited by transepithelial electrical stimulation of hair cells in the sacculus of the bullfrog. Proc Natl Acad Sci U S A. 2003; 100:958–963. [PubMed: 12538849]
38. Martin P, et al. Spontaneous oscillation by hair bundles of the bullfrog's sacculus. J Neurosci. 2003; 23:4533–4548. [PubMed: 12805294]
39. Assad JA, Corey DP. An active motor model for adaptation by vertebrate hair cells. J Neurosci. 1992; 12:3291–3309. [PubMed: 1527581]
40. Howard J, Hudspeth AJ. Mechanical relaxation of the hair bundle mediates adaptation in mechanoelectrical transduction by the bullfrog's saccular hair cell. Proc Natl Acad Sci U S A. 1987; 84:3064–3068. [PubMed: 3495007]
41. Corey DP, Hudspeth AJ. Ionic basis of the receptor potential in a vertebrate hair cell. Nature. 1979; 281:675–677. [PubMed: 45121]
42. Ohmori H. Mechano-electrical transduction currents in isolated vestibular hair cells of the chick. J Physiol. 1985; 359:189–217. [PubMed: 2582113]
43. Beurg M, et al. A large-conductance calcium-selective mechanotransducer channel in mammalian cochlear hair cells. J Neurosci. 2006; 26:10992–11000. [PubMed: 17065441]
44. Ricci AJ, et al. Tonotopic variation in the conductance of the hair cell mechanotransducer channel. Neuron. 2003; 40:983–990. [PubMed: 14659096]
45. Farris HE, et al. Probing the pore of the auditory hair cell mechanotransducer channel in turtle. J Physiol. 2004; 558:769–792. [PubMed: 15181168]
46. Cueva JG, et al. Nanoscale organization of the MEC-4 DEG/ENaC sensory mechanotransduction channel in Caenorhabditis elegans touch receptor neurons. The Journal of neuroscience : the official journal of the Society for Neuroscience. 2007; 27:14089–14098. [PubMed: 18094248]
47. Kung C, et al. Mechanosensitive channels in microbes. Annual review of microbiology. 2010; 64:313–329.
48. Ahmed ZM, et al. Mutations of the protocadherin gene PCDH15 cause Usher syndrome type 1F. Am J Hum Genet. 2001; 69:25–34. [PubMed: 11398101]
49. Alagramam KN, et al. The mouse Ames waltzer hearing-loss mutant is caused by mutation of Pcdh15, a novel protocadherin gene. Nat Genet. 2001; 27:99–102. [PubMed: 11138007]
50. Alagramam KN, et al. Mutations in the novel protocadherin PCDH15 cause Usher syndrome type 1F. Hum Mol Genet. 2001; 10:1709–1718. [PubMed: 11487575]
51. Bolz H, et al. Mutation of CDH23, encoding a new member of the cadherin gene family, causes Usher syndrome type 1D. Nat Genet. 2001; 27:108–112. [PubMed: 11138009]
52. Bork JM, et al. Usher syndrome 1D and nonsyndromic autosomal recessive deafness DFNB12 are caused by allelic mutations of the novel cadherin-like gene CDH23. Am J Hum Genet. 2001; 68:26–37. [PubMed: 11090341]
53. Di Palma F, et al. Mutations in Cdh23, encoding a new type of cadherin, cause stereocilia disorganization in waltzer, the mouse model for Usher syndrome type 1D. Nat Genet. 2001; 27:103–107. [PubMed: 11138008]
54. Wada T, et al. A point mutation in a cadherin gene, Cdh23, causes deafness in a novel mutant, Waltzer mouse niigata. Biochem Biophys Res Commun. 2001; 283:113–117. [PubMed: 11322776]

55. Wilson SM, et al. Mutations in Cdh23 cause nonsyndromic hearing loss in waltzer mice. Genomics. 2001; 74:228–233. [PubMed: 11386759]
56. Sollner C, et al. Mutations in cadherin 23 affect tip links in zebrafish sensory hair cells. Nature. 2004; 428:955–959. [PubMed: 15057246]
57. Siemens J, et al. Cadherin 23 is a component of the tip link in hair-cell stereocilia. Nature. 2004; 428:950–955. [PubMed: 15057245]
58. Ahmed ZM, et al. The tip-link antigen, a protein associated with the transduction complex of sensory hair cells, is protocadherin-15. J Neurosci. 2006; 26:7022–7034. [PubMed: 16807332]
59. Kazmierczak P, et al. Cadherin 23 and protocadherin 15 interact to form tip-link filaments in sensory hair cells. Nature. 2007; 449:87–91. [PubMed: 17805295]
60. Goodyear RJ, et al. Asymmetric distribution of cadherin 23 and protocadherin 15 in the kinocilial links of avian sensory hair cells. J Comp Neurol. 2010; 518:4288–4297. [PubMed: 20853507]
61. Muller U. Cadherins and mechanotransduction by hair cells. Curr Opin Cell Biol. 2008; 20:557–566. [PubMed: 18619539]
62. Niessen CM, et al. Tissue organization by cadherin adhesion molecules: dynamic molecular and cellular mechanisms of morphogenetic regulation. Physiol Rev. 2011; 91:691–731. [PubMed: 21527735]
63. Shapiro L, Weis WI. Structure and biochemistry of cadherins and catenins. Cold Spring Harb Perspect Biol. 2009; 1:a003053. [PubMed: 20066110]
64. Yagi T, Takeichi M. Cadherin superfamily genes: functions, genomic organization, and neurologic diversity. Genes Dev. 2000; 14:1169–1180. [PubMed: 10817752]
65. Nelson WJ. Regulation of cell-cell adhesion by the cadherin-catenin complex. Biochem Soc Trans. 2008; 36:149–155. [PubMed: 18363555]
66. Oda H, Takeichi M. Evolution: structural and functional diversity of cadherin at the adherens junction. J Cell Biol. 2011; 193:1137–1146. [PubMed: 21708975]
67. Boggon TJ, et al. C-cadherin ectodomain structure and implications for cell adhesion mechanisms. Science. 2002; 296:1308–1313. [PubMed: 11964443]
68. Haussinger D, et al. Proteolytic E-cadherin activation followed by solution NMR and X-ray crystallography. Embo J. 2004; 23:1699–1708. [PubMed: 15071499]
69. Zhang Y, et al. Resolving cadherin interactions and binding cooperativity at the single-molecule level. Proc Natl Acad Sci U S A. 2009; 106:109–114. [PubMed: 19114658]
70. Patel SD, et al. Type II cadherin ectodomain structures: implications for classical cadherin specificity. Cell. 2006; 124:1255–1268. [PubMed: 16564015]
71. Elledge HM, et al. Structure of the N terminus of cadherin 23 reveals a new adhesion mechanism for a subset of cadherin superfamily members. Proc Natl Acad Sci U S A. 2010; 107:10708–10712. [PubMed: 20498078]
72. Sotomayor M, et al. Structural determinants of cadherin-23 function in hearing and deafness. Neuron. 2010; 66:85–100. [PubMed: 20399731]
73. Katsamba P, et al. Linking molecular affinity and cellular specificity in cadherin-mediated adhesion. Proc Natl Acad Sci U S A. 2009; 106:11594–11599. [PubMed: 19553217]
74. Chen CP, et al. Specificity of cell-cell adhesion by classical cadherins: Critical role for low-affinity dimerization through beta-strand swapping. Proc Natl Acad Sci U S A. 2005; 102:8531–8536. [PubMed: 15937105]
75. Pokutta S, et al. Conformational changes of the recombinant extracellular domain of E-cadherin upon calcium binding. European journal of biochemistry/FEBS. 1994; 223:1019–1026. [PubMed: 8055942]
76. Harrison OJ, et al. The extracellular architecture of adherens junctions revealed by crystal structures of type I cadherins. Structure. 2011; 19:244–256. [PubMed: 21300292]
77. Wu Y, et al. Transforming binding affinities from three dimensions to two with application to cadherin clustering. Nature. 2011; 475:510–513. [PubMed: 21796210]
78. Wu Y, et al. Cooperativity between trans and cis interactions in cadherin-mediated junction formation. Proc Natl Acad Sci U S A. 2010; 107:17592–17597. [PubMed: 20876147]

79. Kachar B, et al. High-resolution structure of hair-cell tip links. Proc Natl Acad Sci U S A. 2000; 97:13336–13341. [PubMed: 11087873]
80. Sotomayor M, Schulten K. The allosteric role of the Ca2+ switch in adhesion and elasticity of C-cadherin. Biophys J. 2008; 94:4621–4633. [PubMed: 18326636]
81. Oroz J, et al. Nanomechanics of the cadherin ectodomain: “canalization” by Ca2+ binding results in a new mechanical element. J Biol Chem. 2011; 286:9405–9418. [PubMed: 21177864]
82. Bosher SK, Warren RL. Very low calcium content of cochlear endolymph, an extracellular fluid. Nature. 1978; 273:377–378. [PubMed: 661948]
83. Salt AN, et al. Calcium gradients in inner ear endolymph. Am J Otolaryngol. 1989; 10:371–375. [PubMed: 2596623]
84. Schwander M, et al. A mouse model for nonsyndromic deafness (DFNB12) links hearing loss to defects in tip links of mechanosensory hair cells. Proc Natl Acad Sci U S A. 2009; 106:5252–5257. [PubMed: 19270079]
85. Tolomeo JA, et al. Mechanical properties of the lateral cortex of mammalian auditory outer hair cells. Biophys J. 1996; 71:421–429. [PubMed: 8804625]
86. Siemens J, et al. The Usher syndrome proteins cadherin 23 and harmonin form a complex by means of PDZ-domain interactions. Proc Natl Acad Sci U S A. 2002; 99:14946–14951. [PubMed: 12407180]
87. Webb SW, et al. Regulation of PCDH15 function in mechanosensory hair cells by alternative splicing of the cytoplasmic domain. Development. 2011; 138:1607–1617. [PubMed: 21427143]
88. Verpy E, et al. A defect in harmonin, a PDZ domain-containing protein expressed in the inner ear sensory hair cells, underlies Usher syndrome type 1C. Nat Genet. 2000; 26:51–55. [PubMed: 10973247]
89. Weil D, et al. Defective myosin VIIA gene responsible for Usher syndrome type 1B. Nature. 1995; 374:60–61. [PubMed: 7870171]
90. Weil D, et al. Usher syndrome type I G (USH1G) is caused by mutations in the gene encoding SANS, a protein that associates with the USH1C protein, harmonin. Hum Mol Genet. 2003; 12:463–471. [PubMed: 12588794]
91. Caberlotto E, et al. Usher type 1G protein sans is a critical component of the tip-link complex, a structure controlling actin polymerization in stereocilia. Proc Natl Acad Sci U S A. 2011; 108:5825–5830. [PubMed: 21436032]
92. Johnson KR, et al. Mouse models of USH1C and DFNB18: phenotypic and molecular analyses of two new spontaneous mutations of the Ush1c gene. Hum Mol Genet. 2003; 12:3075–3086. [PubMed: 14519688]
93. Lefevre G, et al. A core cochlear phenotype in USH1 mouse mutants implicates fibrous links of the hair bundle in its cohesion, orientation and differential growth. Development. 2008; 135:1427–1437. [PubMed: 18339676]
94. Self T, et al. Shaker-1 mutations reveal roles for myosin VIIA in both development and function of cochlear hair cells. Development. 1998; 125:557–566. [PubMed: 9435277]
95. Senften M, et al. Physical and functional interaction between protocadherin 15 and myosin VIIa in mechanosensory hair cells. J Neurosci. 2006; 26:2060–2071. [PubMed: 16481439]
96. Adato A, et al. Interactions in the network of Usher syndrome type 1 proteins. Hum Mol Genet. 2005; 14:347–356. [PubMed: 15590703]
97. Bahloul A, et al. Cadherin-23, myosin VIIa and harmonin, encoded by Usher syndrome type I genes, form a ternary complex and interact with membrane phospholipids. Hum Mol Genet. 2010; 19:3557–3565. [PubMed: 20639393]
98. Boeda B, et al. Myosin VIIa, harmonin and cadherin 23, three Usher I gene products that cooperate to shape the sensory hair cell bundle. Embo J. 2002; 21:6689–6699. [PubMed: 12485990]
99. Pan L, et al. Assembling stable hair cell tip link complex via multidentate interactions between harmonin and cadherin 23. Proc Natl Acad Sci U S A. 2009; 106:5575–5580. [PubMed: 19297620]
100. Reiners J, et al. Photoreceptor expression of the Usher syndrome type 1 protein protocadherin 15 (USH1F) and its interaction with the scaffold protein harmonin (USH1C). Mol Vis. 2005; 11:347–355. [PubMed: 15928608]

101. Wu L, et al. Structure of MyTH4-FERM domains in myosin VIIa tail bound to cargo. Science. 2011; 331:757–760. [PubMed: 21311020]
102. Yan J, et al. The structure of the harmonin/sans complex reveals an unexpected interaction mode of the two Usher syndrome proteins. Proc Natl Acad Sci U S A. 2010; 107:4040–4045. [PubMed: 20142502]
103. Furness DN, Hackney CM. Cross-links between stereocilia in the guinea pig cochlea. Hear Res. 1985; 18:177–188. [PubMed: 4044419]
104. Michalski N, et al. Harmonin-b, an actin-binding scaffold protein, is involved in the adaptation of mechanoelectrical transduction by sensory hair cells. Pflugers Arch. 2009; 459:115–130. [PubMed: 19756723]
105. Garcia JA, et al. Localization of myosin-Ibeta near both ends of tip links in frog saccular hair cells. J Neurosci. 1998; 18:8637–8647. [PubMed: 9786971]
106. Steyger PS, et al. Myosin Ibeta is located at tip link anchors in vestibular hair bundles. J Neurosci. 1998; 18:4603–4615. [PubMed: 9614235]
107. Holt JR, et al. A chemical-genetic strategy implicates myosin-1c in adaptation by hair cells. Cell. 2002; 108:371–381. [PubMed: 11853671]
108. Schneider ME, et al. A new compartment at stereocilia tips defined by spatial and temporal patterns of myosin IIIa expression. J Neurosci. 2006; 26:10243–10252. [PubMed: 17021180]
109. Kros CJ, et al. Reduced climbing and increased slipping adaptation in cochlear hair cells of mice with Myo7a mutations. Nat Neurosci. 2002; 5:41–47. [PubMed: 11753415]
110. Hasson T. Unconventional myosins, the basis for deafness in mouse and man. Am J Hum Genet. 1997; 61:801–805. [PubMed: 9382088]
111. Grati M, Kachar B. Myosin VIIa and sans localization at stereocilia upper tip-link density implicates these Usher syndrome proteins in mechanotransduction. Proc Natl Acad Sci U S A. 2011; 108:11476–11481. [PubMed: 21709241]
112. Stepanyan R, et al. Auditory mechanotransduction in the absence of functional myosin-XVa. J Physiol. 2006; 576:801–808. [PubMed: 16973713]
113. Stepanyan R, Frolenkov GI. Fast adaptation and Ca2+ sensitivity of the mechanotransducer require myosin-XVa in inner but not outer cochlear hair cells. J Neurosci. 2009; 29:4023–4034. [PubMed: 19339598]
114. Goodyear RJ, et al. Development and properties of stereociliary link types in hair cells of the mouse cochlea. J Comp Neurol. 2005; 485:75–85. [PubMed: 15776440]
115. Reiners J, et al. Molecular basis of human Usher syndrome: deciphering the meshes of the Usher protein network provides insights into the pathomechanisms of the Usher disease. Exp Eye Res. 2006; 83:97–119. [PubMed: 16545802]
116. Hasson T, et al. Unconventional myosins in inner-ear sensory epithelia. J Cell Biol. 1997; 137:1287–1307. [PubMed: 9182663]
117. Harrison OJ, et al. Two-step adhesive binding by classical cadherins. Nat Struct Mol Biol. 2010; 17:348–357. [PubMed: 20190754]

Box 1

Outstanding questions

- What is the molecular identity of the mechanotransduction channel?
- What are the mechanical properties of tip links, and what is the atomic structure of the adhesion interface between CDH23 and PCDH15?
- Which molecule(s) form the gating spring for the transducer channel?
- What is the mechanism of fast adaptation?
- What is the mechanism of slow adaptation and what roles do Myo1c and Myo7a play in this process? Are other myosin motor proteins involved?
- What is the full complement of proteins at the upper and lower end of tip links and how do they regulate tip-link function in mechanotransduction?
- How is the exquisite polarity of CDH23 and PCDH15 at tip links achieved, and how are proteins such as the transduction channel and harmonin targeted to opposite ends of the tip link?
- Which mechanisms define the numbers and rows of stereocilia and their organ pipe arrangement? Which signaling mechanisms establish precise polarity of the hair bundle in the apical surface of a hair cell?

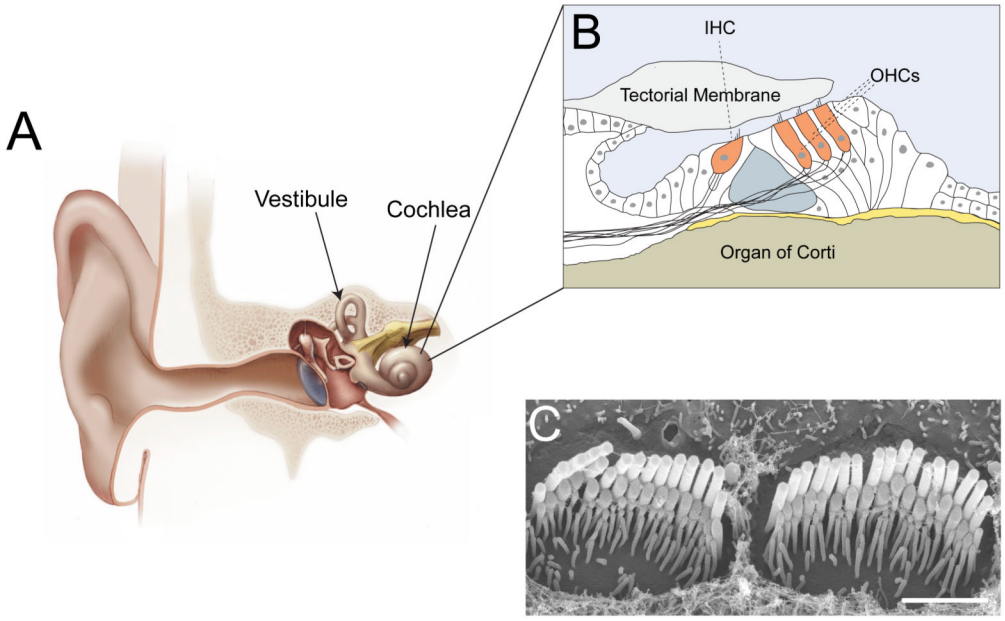

Fig. 1. The mammalian auditory sense organ and its hair cells

(A) Diagram of the inner ear. The snail-shaped cochlea (end organ for the perception of sound) and parts of the vestibule (end organ for the perception of head movement) are indicated (panel modified from [4]). (B) Diagram of the organ of Corti. One inner hair cell (IHC) and three outer hair cells (OHCs) are indicated. (C) Scanning electron micrograph of the cochlear sensory epithelium of the mouse after removal of the tectorial membrane (kindly provided by Dr. Nicolas Grillet, TSRI). The image shows the stereociliary bundles of two IHCs. Note the staircase arrangement of the rows of stereocilia. Scale bar: 2 μm.

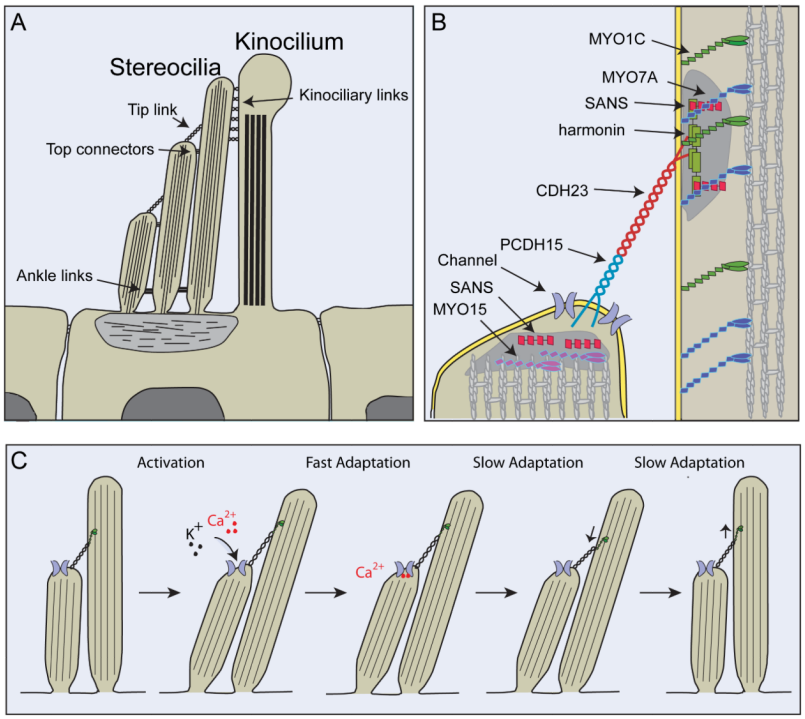

Fig. 2. Hair cells and their mechanotransduction machinery

(A) Cross section through the apical part of a hair cell. Hair bundles consist of several rows of actin-rich stereocilia and a microtubule-based kinocilium. The sterocilia are connected to each other and to the kinocilium by extracellular filaments that can be visualized by electron microscopy. These are the tip links, top connectors, ankle links and kinociliary links (for a recent review see [4]). Note that the kinocilium, kinociliary links, ankle links and top connectors are present in murine cochlear hair cells only during hair bundle development. These structures degenerate once hair bundles have reached their mature shape and only stereocilia, tip links and top connectors remain [114]. (B) Diagram of the tip-link region, indicating molecules that are part of the tip-link complex. CDH23 homodimers form the upper part of the tip link and PCDH15 homodimers the lower part [59]. Two electron dense regions (shaded in gray) can be visualized by transmission electron microscopy in proximity to the upper and lower insertion sites of tip links [103]. Immunolocalization studies have localized the indicated proteins to the electron dense regions (for a recent review see [4]). (C) Current model of activation and adaptation of transduction channels in hair cells. Transduction channels that are located in proximity to the lower insertion site of tip links are opened by deflection of the hair bundle in the direction of the longest sterocilia. The tip link is thought to gate the channel. Ca^{2+} that flows into the stereocilia leads to fast adaptation likely by binding to the channel or a molecule nearby. Slow adaptation is thought to be regulated by a myosin motor complex at the upper insertion site of tip links. Upon Ca^{2+} entry, the adaptation motor is released from the cytoskeleton and slips down the actin filaments, leading to channel closure. Tension in the transduction complex is restored by movement of the myosin motor towards the tips of stereocilia (for a recent review see [1]). However, the localization of the transduction channel raises questions regarding models of slow adaptation because it places the site of Ca^{2+} entry into stereocilia at the lower tip-link end, far away from the proposed localization of the adaptation motor at the upper tip-link end. It has been proposed that Ca^{2+} entering through the transduction channel might affect the adaptation motor hooked up to the next tip link lower down in the same stereocilium [1],

but adaptation motors in the longest stereocilia would then likely not show Ca^{2+}-dependent adaptation.

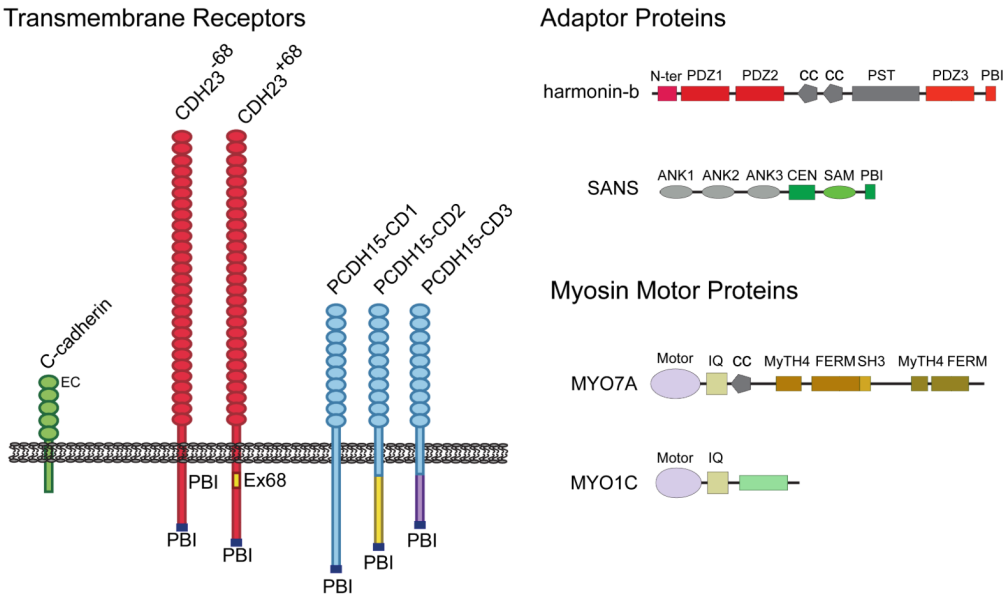

Fig. 3. Molecules of transduction

The domain structure of proteins that have been implicated as components of the tip-link complex are indicated and can be grouped into three categories: 1) transmembrane receptors of the cadherin superfamily (CDH23 and PCDH15) that form tip-link filaments [57-59]. The classical C-cadherin is shown for comparison to the tip-link cadherins. Note that the extracellular domains of CDH23 and PCDH15 are substantially larger than those of classical cadherins. The figure also shows different isoforms of CDH23 and PCDH15 that differ in their cytoplasmic domains. Two CDH23 isoforms have been identified in hair cells that are generated by alternative splicing of exon 68 [57, 86]. For PCDH15, three prominent isoforms that are generated by alternative splicing (PCDH15-CD1, -CD2, and -CD3) are expressed in hair cells [58, 87]. All CDH23 and PCDH15 isoforms contain consensus-binding sites for PDZ domain proteins (PBIs) (for a recent review see [61]). Which isoform of CDH23 and PCDH15 is at tip links remains to be determined; 2) adaptor proteins harmonin and sans. These adaptor proteins bind to the cytoplasmic domains of tip-link cadherins [86, 95-98, 115]. Harmonin can bind to the CDH23 and PCDH15 cytoplasmic domains but it co-localizes at tip links only with CDH23 [29]. Sans can bind to CDH23 and has been localized to the upper and lower ends of tip [91, 111]; 3) myosin motor proteins that are implicated in slow adaptation. Myo1c and Myo7a have been localized to the upper end of tip links but have also been reported, depending on species and experimental conditions, to be more broadly distributed in hair cells [105, 106, 108, 111, 116]. Abbreviations are as follows: Ank, ankyrin-like repeat; cc, coiled-coil domain; CEN, central sans domain; EC, extracellular cadherin repeat; FERM, protein 4.1, ezrin, radixin, moesin domain; IQ, calmodulin binding IQ domain; MyTH4, myosin tail homology 4 domain; N-ter, N-terminal domain of harmonin; PBI, PDZ binding interface; PDZ, PSD95/SAP90, Discs large, zonula occludens-1 domain; PST, proline, serine, threonine rich domain; SAM, sterile alpha motif domain; SH3, src homology 3 domain.

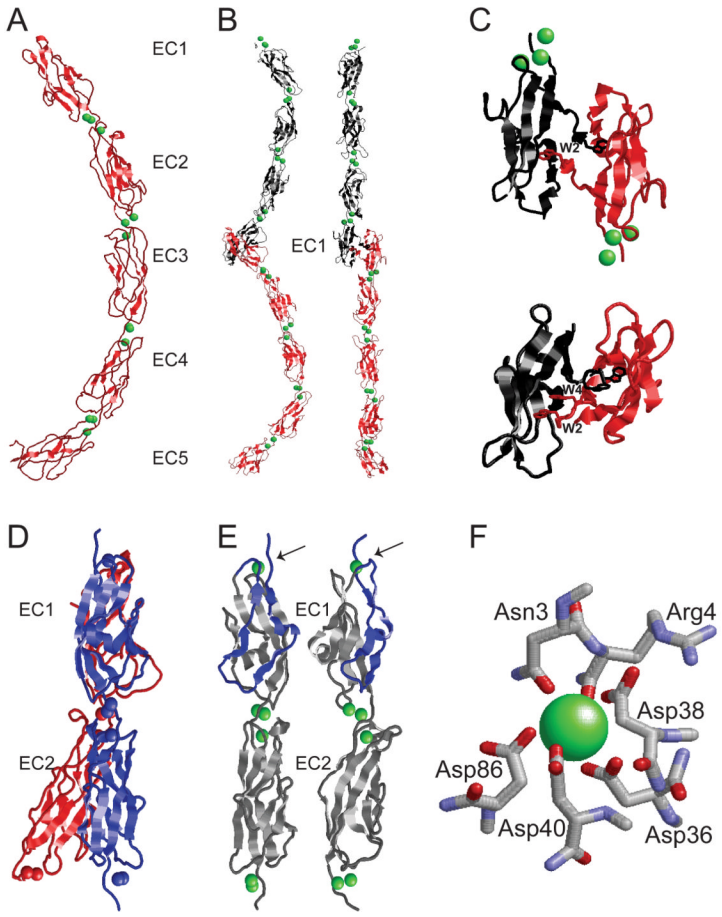

Figure 4. Structural features of the extracellular domains of classical cadherins and Cdh23

The figures summarize crystallographic data for classical cadherins and tip-link cadherins. (A) The entire *Xenopus laevis* C-cadherin extracellular domain (red) in the Ca^{2+} (green) bound state is shown. Note the five extracellular cadherin repeats (EC1-5), the three Ca^{2+} ions that are bound between each of the EC domains, and the curvature of the ectodomain [67]. (B) Adhesive trans dimer of murine E-cadherin [117]. Individual E-cadherin extracellular domains (red and black) emanate from opposing directions. The trans binding surface is located in the EC1 domain. Side view (left) reveals the characteristic curvature of the monomers, which appear straight when rotated by 90° (right). (C) The N-terminal EC1 domains of classical cadherins that engage in trans-interactions are depicted. The molecules form the so-called strand-swapped dimers. Classical type I cadherins such as murine E-cadherin (upper) contain in EC1 one key tryptophan residue (W2) that fits into a binding pocket in EC1 of its binding partner [117]. Classical type II cadherins such as murine MN-cadherin (lower) contain two tryptophan residues (W2 and W4) that fit into two binding pockets on EC1 of the binding partner [70]. (D) Crystallographic structure of the EC1-EC2 domain of murine CDH23 (blue) [71, 72]. The classic cadherin fold with Ca^{2+} ions (blue dots) between EC1 and EC2 is maintained. Superimposition of EC1-EC2 of C-cadherin (red) highlights the straight alignment of CDH23 EC1-EC2 compared to the curvature of C-cadherin [67, 71]. (E) Structure of the EC1-EC2 domains of two parallel CDH23 molecules. Note that only monomeric structures have been crystallized. The contact surface between EC domains that are aligned in parallel remain to be determined. Ca^{2+} ions (green dots) are indicated. Note the presence of a Ca^{2+} ion at the extreme N-terminus of CDH23 that is not bound by classical cadherins. The strands formed by amino acids 1-4 are clamped down in a

loop (blue) by the coordinate bond between Asn3, Arg4, Asp36, Asp38, Asp40 and Ca^{2+} to form a large exposed area on the surface of EC1. Mutations in Asn3 and Arg4 reduce CDH23 binding to PCDH15 [71]. (F) Detailed view of the amino acids in CDH23 that coordinate the N-terminal Ca^{2+} [71, 72]. Structures were generated in RasMol (http://www.umass.edu/microbio/rasmol/) using protein coordinates from the Protein Data Bank (PDB) database (www.pdb.org).

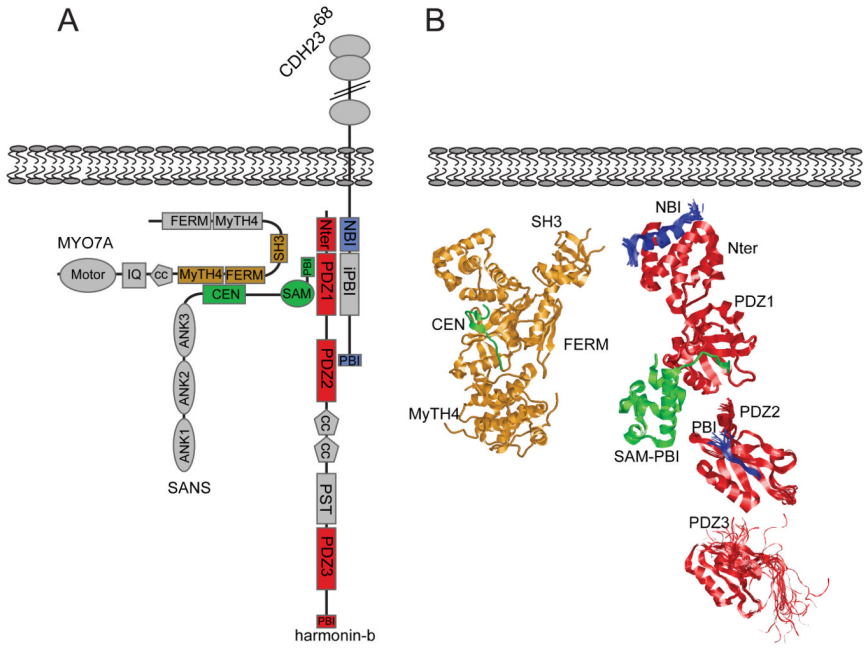

Figure 5. Structural aspects of the UTLD complex emerging from crystallographic and biochemical studies

(A,B) Model of the interactions between proteins at the UTLD. In (A) a model of the interaction surfaces is provided that is based on biochemical data and, where available, on structural information [86, 95-102]. In (B), the known crystal structures are shown, except for an internal binding motif for PDZ-domain proteins (NBI) of CDH23, which was fitted artificially into its N-terminal binding site on harmonin. Protein-domains in (A) are color-coded to match the structures in (B). Abbreviations are as in Figure 3. Note that we present here a partial representation not considering all interactions revealed by biochemical data. For example, Myo7a can also bind to harmonin and CDH23 [94, 106], but these complexes have not yet been crystallized. Structures were generated as described in Figure 4.